LETTERS

HIGH-ENERGY RUNAWAY ORBITS IN THE PRESENCE OF AN m = 2 MAGNETIC ISLAND

S.J. ZWEBEN[a], B.V. WADDELL[b], D.W. SWAIN (Oak Ridge National Laboratory, Oak Ridge, Tennessee), H.H. FLEISCHMANN (Cornell University, Ithaca, New York, United States of America)

ABSTRACT. A guiding-centre computer code is used to map out trajectories of collisionless high-energy runaways in the presence of an m = 2 magnetic island in a tokamak. The particle drift surfaces retain the island structure even when the drift orbits are considerably shifted from the flux surfaces, and trapped-particle orbits are observed to be unaffected by the presence of the island.

1. INTRODUCTION

There is a growing body of evidence for the existence of m = 2 magnetic islands inside tokamaks [1, 2]. It is clear that low-energy particle drift surfaces will tend to follow these perturbed flux surfaces, but it is not as yet clear how the drift orbits of high-energy collisionless particles are affected by the presence of such structures. Does the usual shift of the high-energy particle drift surfaces from the flux surfaces destroy the island structure in the particle orbit? The question is of interest for the confinement properties of high-energy runaways, and perhaps also for neutral-beam-injected ions or fusion-produced α-particles which can also have large orbit shifts and are fairly collisionless.

The structure of magnetic islands in tokamaks has been studied extensively. Chrisman, Clarke and Rome [3] showed that helical sheet current perturbations in a cylindrical tokamak geometry can produce islands in the flux surfaces and proposed a connection between the observed modulation of hard-X-ray emission for ORMAK and these perturbed flux surfaces. Finn [4] and Waddell et al. [5] (among others) have studied the sensitivity of island structures to variations in the assumed plasma current profile and have proposed as a mechanism for the major disruption the non-linear coupling between different m-mode islands.

Karger et al. [1] have experimentally studied the correlation between periodic hard-X-ray emission from the Pulsator limiter and the m = 2 island appearing before disruption and have postulated that a loss of high-energy ($\lesssim 8$ MeV) runaways before the main disruptive voltage spike was due to the outward shift of these particles. Observations on ATC and other tokamaks [6] have also shown that large-amplitude MHD oscillations (without disruption) can also modulate and enhance the loss of runaways.

Recently, Fussmann et al. [7] have extended the Pulsator work both experimentally and theoretically. In particular, they have calculated guiding-centre trajectories of runaway orbits in the presence of an approximately m = 1, n = 1 external magnetic perturbation. Our results described below are qualitatively consistent with those of Fussmann et al. in that an island structure in the runaway drift orbit is observed even though the orbits are shifted from magnetic-flux surfaces. However, our results supplement and extend theirs at the following points:

1) We have used an internal m = 2 helical perturbation instead of the external (stellarator-type) perturbation of Ref. [7]. This internal perturbation was chosen to fit the best available information on the internal structure of the m = 2 island in the tokamak. In addition, we have used a realistic plasma current profile instead of an axial filament current profile as in Ref. [7].
2) We find that trapped-particle collisionless orbits are unaffected by the magnetic island (only passing particle orbits were reported in Ref. [7]).
3) We have followed the time-dependent runaway orbit by including a parallel electric field, and find that these orbits are simply related to the time-independent ones (as calculated in Ref. [7]).

In the following analysis, we calculate collisionless runaway drift orbits in the presence of an m = 2 magnetic island structure which is considered to be stationary on the time scale of a runaway toroidal transit (typically, ~ 50 ns). Such runaway drift surfaces would tend to remain locked in phase with respect to the slowly rotating ($f \approx 10$ kHz) island, presumably causing the observed B_p oscillations to be correlated with hard-X-ray emission from the outer limiter of the tokamak. The effects of a growing or turbulent island structure have not been considered in the present work. The computation of the effect of more than one island on the runaway orbit requires a more complicated formalism and has not been attempted here.

[a] Present address: Tokamak Fusion Laboratory, 2567 Boelter Hall, University of California, Los Angeles, CA 90024, USA.
[b] Deceased.

2. GUIDING-CENTRE CODE

The following simplified set of guiding-centre equations was used to calculate orbits in a standard cylindrical geometry (r, θ, z), with $x = r\cos\theta$, $y = r\sin\theta$, and for an electron with mass m, pitch angle ξ and velocity $\vec{v}$, $v_z = v\cos\xi$ and $v_\perp = v\sin\xi$, and $v_\perp^2 = v_x^2 + v_y^2$:

$$\text{(a)}\quad \frac{dx}{dt} = v_z\left(\frac{B_x}{B_0}\right)\left(\frac{R}{R_0}\right)$$

$$\text{(b)}\quad \frac{dy}{dt} = v_z\left(\frac{B_y}{B_0}\right)\left(\frac{R}{R_0}\right) + v_d$$

$$\text{(c)}\quad \frac{dz}{dt} = v_z \qquad (1)$$

$$\text{(d)}\quad \frac{d(\gamma m_0 v_z)}{dt} = e\,\mathbb{E} - M\frac{\partial B}{\partial s}$$

$$\text{(e)}\quad \frac{d(\gamma m_0 c^2)}{dt} = e\,\mathbb{E}\,v_z$$

where

$$v_d = -\frac{\gamma}{\Omega_0 R_0}\left(v_z^2 + \frac{1}{2}v_\perp^2\right)$$

and

$$M\frac{\partial B}{\partial s} = \left(\frac{\gamma m_0 v_\perp^2}{2R_0}\right)\left(\frac{B_x}{B_0}\right)$$

Here,

$R = R_0 + x = R_0 + r\cos\theta$

$B_z = B_0 R_0/R$ is the axial ('toroidal') magnetic field

$v/c = \sqrt{v_\perp^2 + v_z^2}/c = \sqrt{1 - 1/\gamma^2}$

$\Omega_0 = eB_0/m_0 c$

$M = \gamma m_0 v_\perp^2 R/(2 B_0 R_0)$

$\mathbb{E}$ = electric field along $\hat{z}$

s = arc length along orbit

The following simplifying approximations have been made in the above equations:

1) toroidal geometry is approximated by a periodic cylindrical system (periodicity $2\pi R_0$) in which the axial ('toroidal') magnetic field is $B_z = B_0 R_0/R$;

2) the poloidal field $B_p = (B_x^2 + B_y^2)^{1/2}$ is chosen to be cylindrically symmetric and to be much smaller than the axial field (the usual tokamak ordering);

3) the magnitudes of the cross-field ∇B and the centrifugal drift velocities v_d are evaluated by using only the local unperturbed axial field, ignoring the smaller poloidal field and the still smaller island fields. Thus,

$$v_D = \frac{1}{eB^3}\left(\frac{P_\parallel^2}{\gamma m_0} + \frac{P_\perp^2}{2\gamma m_0}\right) \cong \frac{\gamma}{\Omega_0 R_0}\left(v_z^2 + v_\perp^2/2\right)$$

(see Ref. [8] for the relativistic drift equations).

4) the mirroring term written as $M\partial B/\partial s$, where M is the magnetic moment, is approximated for a relativistic electron as $M = \gamma m_0 v_\perp^2 R/(2 B_0 R_0)$ and $\partial B/\partial s = (B_x/B)(\partial B/\partial x) = -B_x/R$, so that the force is approximately $(\gamma m_0 v_\perp^2/2R_0)(B_x/B_0)$.

The most important feature of these equations in the present context is that the guiding-centre velocity vector tends to point in the direction of the local magnetic field which includes the island fields in the B_x and B_y. It is this which allows the formation of the magnetic islands in the drift surfaces. Of course, the results we obtain using these approximations may be modified to some extent by a more exact treatment of the problem; however, we believe that the basic orbit patterns are valid (within the restrictions described at the end of Section 1).

Left to be specified is the toroidal current distribution which determines the unperturbed poloidal field. We have taken

$$q(r) = \frac{B_0}{B_p}\frac{r}{R} = \frac{m}{nC_1}\left[1 + (r/r_0)^2\right] \qquad (2)$$

to define B_p, where r_0 is a parameter which determines the effective width of the current channel, and $C_1 = 1 + (r_s/r_0)^2$, where r_s is the radius of the singular surface (m, n). Normalizing all radii to the limiter radius a, we have typically for m = 2, n = 1: $\hat{r}_0 = r_0/a = 0.8$, $\hat{r}_s = r_s/a = 0.6$; thus, $q(a) = 3.3$ and $q(0) = 1.3$.

This set of five coupled differential equations has been solved numerically by using a well-documented computer code (ODE). It is found that the code reproduces the usual particle orbits with a shift $d_\gamma \cong (a^2/2R_0)(I_A/I) \propto \gamma/B_p$ of high energy electrons from the flux surfaces [9] (here, $I_A \cong 17\gamma$ kA, and I is the current producing B_p) and also produces the usual banana orbits for large ξ. Particle orbits in this field structure (without islands) can be followed for many hundreds of toroidal transits without a noticeable wandering from the initial drift surfaces.

3. m = 2 ISLAND PERTURBATION

An m = 2 magnetic island has been included into the code by adding to Eq. (1) the perturbed poloidal fields B_{x1} and B_{y1} due to the island. Since these m = 2, n = 1 fields are much smaller than B_0, no change in the particle drift velocity v_d has been made; the effect of the island, therefore, comes entirely through the tendency of the guiding centre to follow the perturbed magnetic field line.

The perturbed fields are obtained from an analytic fit to a saturated m = 2 island structure as calculated by using the 2-D MASS code [10]. A helical flux function ψ is defined in a cylindrical co-ordinate system:

$$B_r = \frac{1}{r}\frac{\partial \Psi}{\partial \theta}$$

$$B_\theta = -\frac{\partial \Psi}{\partial r} - \frac{kr}{m} B_z \quad (k \equiv n/R_0) \tag{3}$$

$$B_z = \text{constant}$$

It is easy to verify that the unperturbed field given by Eq. (2) can be written in terms of a normalized $\hat{\Psi}_0 = \Psi_0/(a^2 k B_z/m)$ and a normalized $\hat{r} = r/a$ as follows:

$$\hat{\Psi}_0(\hat{r}) = C_3 \ln\left[1 + (\hat{r}/\hat{r}_0)^2\right] - \frac{1}{2}\hat{r}^2 + C_2 \tag{4}$$

where

$$C_3 = \frac{1}{2}\hat{r}_0^2\left[1 + (\hat{r}_s^2/\hat{r}_0^2)\right]$$

and

$$C_2 = -C_3 \ln\left(1 + \hat{r}_0^{-2}\right) + \frac{1}{2}$$

The perturbed helical flux $\hat{\Psi}_1(r, \theta, z)$ for the island has been taken from a fit to the numerical results of the MASS code to be:

$$\hat{\Psi}_1 = C_4 \hat{r}^2 \exp\left[-(\hat{r}-\alpha\hat{r}_s)^2/\hat{w}^2\right](1-\hat{r})\cos(2\theta + kz) \tag{5}$$

where $\hat{w} = w/a$ is the normalized width of the m = 2, n = 1 island, and

$$C_4 = \frac{\hat{w}}{16 f(\hat{r}_s, \hat{w})}\left[\frac{\hat{r}_s^2/\hat{r}_0^2}{1 + (\hat{r}_s^2/\hat{r}_0^2)}\right] \tag{6}$$

with

$$f(\hat{r}_s, \hat{w}) = \hat{r}_s^2 \exp\left(\frac{-\hat{r}_s^2}{\hat{w}^2}\right)(1 - \hat{r}_s) \tag{7}$$

The island is, therefore, specified by choosing $\hat{r}_s$ (the radius of the m = 2 singular surface), $\hat{w}$ (the width of the island), and α (a parameter which slightly affects the centring of the flux surfaces within the island). It can be checked that $\vec{B} \cdot \nabla\hat{\Psi} = 0$; thus, a magnetic field line lies on a helical flux surface of constant $\hat{\Psi}$.

The perturbed magnetic fields $B_1(r, \theta)$ corresponding to this island can be found through Eq. (3). These fields are added to the unperturbed fields to form the m = 2 magnetic structure. It is important to note that both the poloidal and radial components of B_1 are added into the code.

4. DRIFT ORBITS WITH m = 2 ISLAND

In Fig.1 we show a typical result for a set of runs in which the runaway energy was varied to show the effect of the shift d_γ on the drift orbit. Here, M = 0, $\mathbb{E}$ = 0, and the island perturbation was the same for all cases ($\hat{w} = 0.4$). Each dot in these graphs is the puncture of a fixed z = constant plane by the particle orbit. The drift surfaces for $\gamma \approx 1$ are, as expected, identical with a direct plot of the flux surfaces. For higher-energy electrons, the drift surfaces are shifted to the right, and it can be seen that the island structure in the drift surfaces is retained until about $d_\gamma \approx w$, at which point the island structure becomes severely distorted and disappears altogether for $d_\gamma/a \gtrsim 0.7$.

Several interesting features of these orbits can be mentioned. First, there appears clearly m = 3 structure somewhere between q = 1 and q = 2 for case (b); this is most likely due to the coupling between the m = 2 island and the m = 1 orbit shift. Secondly, the very-high-energy orbits unexpectedly show both lobes of the m = 2, n = 1 island structure on one side of the minor axis [case (e)]. It should also be noted that the outermost edge of the island in the drift surface can extend at least 0.15a beyond the edge of the island structure in the flux itself [case (c)].

Another set of runs was made in which the magnetic moment was varied by changing ξ for a fixed particle energy and a fixed island structure, and some results are shown in Fig.2. (The orbits in this figure had $d_\gamma/a \sim 0.1$ and were started at a fixed x/a = 0.8, y/a = 0.) For the passing particle orbits in (a) and (b), the drift surfaces show the typical m = 2, n = 1 island

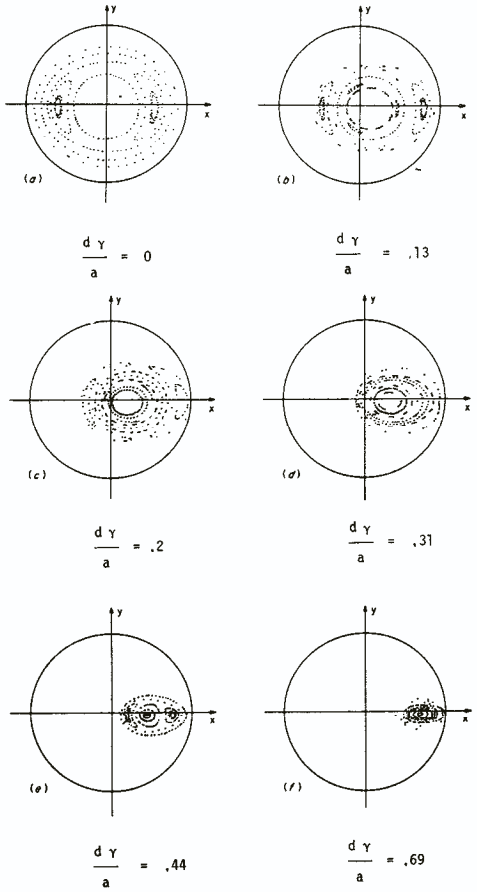

FIG.1. Drift orbits of relativistic electrons in the presence of an m = 2 island. The electron energy (and hence the orbit shift d_γ) is increased from (a) to (f). Only orbits enclosed within the chamber minor radius are shown. Here, M = 0, $\hat{r}_s = 0.6$, $\hat{r}_0 = 0.8$, $\hat{w} = 0.4$, and $\alpha = 0.4$ for all cases.

structure, but for large ξ (e.g. case (d)) the orbit topology changes to that of a normal trapped particle with no trace of an influence from the island (i.e. the orbit is nearly identical with or without the island perturbation added to the field structure). Near the trapping boundary $\xi = 57°$ in case (c) the orbit structure becomes complicated and appears to become ergodic over a limited region. This is the only example of ergodic-type behaviour observed in our results; normal orbits such as those in Figs 1 and 2 have been mapped out for hundreds of transits without showing such a wandering.

The effect of particle acceleration on drift surfaces has also been modelled through the electric field term in Eq. (1). For the case in which no island was put into code, it was found that, as a particle accelerated, its drift orbit gradually shifted away from the flux surfaces without a change in the minor radius of the orbit. When the island perturbation was included, this behaviour was again obtained. This generally meant that an orbit which started out on an island-shaped flux surface retained that structure as the shift increased, i.e. the orbits were just as those shown in Fig.1, given the (approximate) constraint that the orbit minor radius remained unchanged as the particle energy varied.

5. DISCUSSION

We have found in this model that high-energy particle drift surfaces can be shifted considerably from an m = 2 island flux surface and still retain the island topology. It has also been found that trapped-particle orbits are not affected by the island structure,

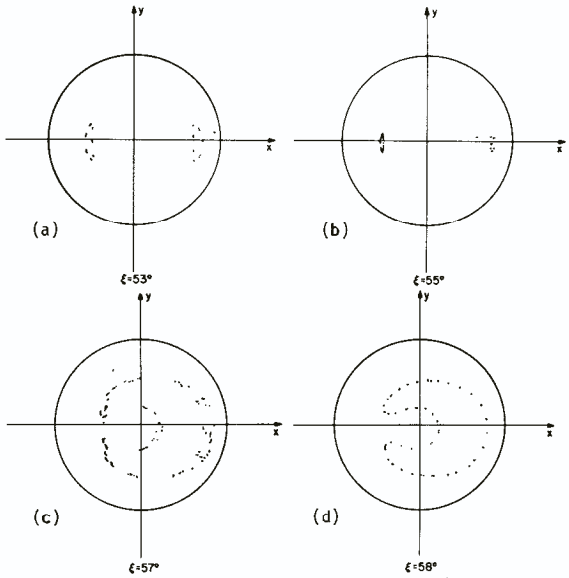

FIG.2. Drift orbits with varying pitch angle ξ in the presence of the same island as for Fig.1. Cases (a) and (b) show the island-shaped drift orbits for passing particles, case (d) shows the absence of the island structure for a trapped-particle orbit. Case (c) shows some ergodicity near the trapping boundary. All orbits here have $d_\gamma = 0.1$ and are started at $x/a = 0.8$, $y/a = 0$.

and that accelerating particle orbits shift from the flux surfaces while roughly retaining their initial minor radius.

The first of these results is consistent with the expectation that a small shift of the drift surfaces from the flux surfaces should not affect the orbit topology. We have found in this model that a shift of $\lesssim 0.15a$ may be considered to be small. However, for larger shifts the topology can change significantly, producing new types of drift orbits such as those shown in Fig.1(e), in which both lobes of the island in the drift surface are on one side of the magnetic axis.

The lack of an island structure for trapped particles is not so unexpected since these particles do not completely resonate with the helical island perturbation. Since this effect is not limited to particles with large orbit shifts, perhaps fluid codes for island growth need to be modified to include this fact.

The accelerating particle orbits are seen to be closely related to the time-independent orbits. This is likely to be connected with the statement that the cross-sectional area of closed runaway orbits is an adiabatic invariant with respect to particle energy variations [7].

There are several considerations, both theoretical and experimental, which need to be elaborated before a comparison of observed runaway confinement with this model can be attempted. Qualitatively, it is clear that the modulation of runaway loss at the outer limiter shows that the confinement of these particles is affected by the m = 2 mode. A quantitative explanation of this phenomenon needs to take into account at least the following points:

1) The model used here of a single m = 2 island ignores effects due to the possible coupling with other modes (e.g. the m = 1) and, in particular, ignores the possibility that such coupling may cause stochasticity in the fine structure of the orbits. Thus the effect on runaway confinement could depend significantly on the size of the island perturbation [6] and on the current profile which in part determine the extent of the coupling.

2) The experimental observations of runaway loss at the outer limiter are in general not sufficient to define the transport of runaways within the plasma. For example, a simple kink-mode magnetic structure might also produce the modulation of runaway flux to the limiter. Also, a quantitative analysis of runaway confinement requires a knowledge of their production rate inside the plasma (which cannot be determined with precision experimentally) and also an energy-resolved runaway diagnostic (since many energy components are intersecting the outer limiter simultaneously).

3) The implications of even our simple model described here have not been mapped completely; for example, the long-time behaviour of the orbits and the ergodic behaviour observed near the trapping boundary can be explored more fully.

It should, therefore, be stressed that it is quite difficult to determine the magnetic structure of the tokamak through a study of runaway confinement. Clearly, the experimental results of the Pulsator group [1, 7] concerning the modulation of the runaway flux at the limiter, and the previous experiments on runaway diffusion [11], have been somewhat ambiguous with respect to their theoretical interpretation. For this reason, the present work is not intended to explain the experimental results, but rather to add to the understanding of this particular theoretical model.

ACKNOWLEDGEMENTS

The authors thank H.E. Knoepfel, J.A. Rome, and D.A. Spong for valuable suggestions.

REFERENCES

[1] KARGER, F., LACKNER, K., FUSSMANN, G., CANNICI, B., ENGELHARDT, W., GERNHARDT, G., GLOCK, E., GROENING, D.E., KLÜBER, O., LISITANO, G., MAYER, H.M., MEISEL, D., MORANDI, P., SESNIC, S., WAGNER, F., ZEHRFELD, H.P., in Plasma Physics and Controlled Nuclear Fusion Research (Proc. 6th Int. Conf. Berchtesgaden, 1976) Vol. 1, IAEA, Vienna (1977) 267.

[2] SAUTOFF, N., VON GOELER, S., STODIEK, W., Nucl. Fusion **18** (1978) 445.

[3] CHRISMAN, P., CLARKE, J.F., ROME, J.A., ORNL Report ORNL/TM-4501 (Mar. 1974).

[4] FINN, J.M., Nucl. Fusion **15** (1975) 845.

[5] WADDELL, B.V., CARRERAS, B., HICKS, H.R., HOLMES, J.A., LEE, D.K., Phys. Rev. Lett. **41** (1978) 1386.

[6] BOYD, D.A., STAUFFER, F.J., TRIVELPIECE, A.W., Phys. Rev. Lett. **37** (1975) 98; HUTCHINSON, I.H., MORTON, A.H., Nucl. Fusion **16** (1976) 447.

[7] FUSSMANN, G., ENGELHARDT, W., FENEBERG, W., GERNHARDT, J., GLOCK, E., KARGER, F., SESNIC, S., ZEHRFELD, H.P., in Plasma Physics and Controlled Nuclear Fusion Research (Proc. 7th Int. Conf. Innsbruck, 1978) Vol. 1, IAEA, Vienna (1979) 401.

[8] NORTHRUP, T.G., Adiabatic Motion of Charged Particles, Interscience (1963).
[9] KNOEPFEL, H.E., ZWEBEN, S.J., Phys. Rev. Lett. 35 (1975) 1340.
[10] WHITE, R.B., MONTICELLO, D.A., ROSENBLUTH, M.N., WADDELL, B.V., in Plasma Physics and Controlled Nuclear Fusion Research (Proc. 6th Int. Conf. Berchtesgaden, 1976) Vol. 1, IAEA, Vienna (1977) 569.
[11] STRACHAN, J.D., Nucl. Fusion 17 (1977) 141; ZWEBEN, S.J., SWAIN, D.W., FLEISCHMANN, H.H., Nucl. Fusion 18 (1978) 1679.

(Manuscript received 10 July 1979
Final manuscript received 12 December 1979)

STABILITY OF DRIFT-WAVE EIGENMODES WITH ARBITRARY RADIAL WAVELENGTHS

Y.C. LEE (Department of Physics, University of California, Los Angeles, California, USA), L. CHEN, W.M. NEVINS* (Plasma Physics Laboratory, Princeton University, Princeton, New Jersey, USA)

ABSTRACT. A general theory for the stability of collisionless drift-wave eigenmodes in sheared slab magnetic fields is developed using the S-matrix technique. The eigenmodes are described with the integral formulation which fully takes into account the non-local effects of finite ion gyro-orbits. The universal eigenmode is then shown to be absolutely stable for arbitrary radial wavelengths.

Recently, significant progress [1] has been made in understanding the stability properties of drift-wave eigenmodes in a sheared magnetic field and slab geometry within the second-order *differential* eigenmode equation formulation. However, the differential formulation is justified only when the radial wavelengths are much longer than the ion-Larmor radius ($|\rho_i^2 d^2/dx^2| \ll 1$). For the case of cold ions ($T_i \ll T_e$), the ion-sonic turning points of Pearlstein and Berk [2] are much closer to the mode-rational surface ($\vec{k} \cdot \vec{B} = 0$) than are the regions of heavy ion-Landau damping and, hence, determine the radial scale length of the drift-wave eigenmode. Then the simple WKB estimate $k_x \sim (L_n T_i / L_s T_e)^{1/2} / \rho_i$ (where L_n and L_s are the density and magnetic shear scale lengths) shows that the long radial wavelength assumption is valid here. For $T_e \sim T_i$, the WKB estimate $k_x \rho_i \sim (L_n/L_s)^{1/2}$ still holds for long azimuthal wavelength modes propagating in the electron diamagnetic drift direction. However, at shorter azimuthal wavelengths ($k_y \rho_i > 1$), the radial localization of the eigenmode is determined by ion-Landau damping and the radial wavelengths become of the order of the ion-Larmor radius, so that the usual differential eigenmode equation ceases to be valid. For eigenmode travelling in the ion diamagnetic direction, the differential formulation is, in general, not at all valid because of the importance of ion-Landau damping for this kind of mode. Moreover, experimentally observed drift-wave fluctuations [3] tend to have wavelengths shorter than the ion-Larmor radius. Therefore, to assess the stability properties of short-wavelength drift-wave eigenmodes correctly, it is necessary to take into account explicitly the non-local nature of ion gyro-orbits through an *integral* eigenmode equation formulation [4]. This is particularly important because the differential formulation predicts the existence of very weakly damped eigenmodes. Hence, it would appear that any small additional effect might give rise to absolute instabilities. Although there have been some numerical efforts [5] in this direction, we believe that this letter is the first such analytical treatment. Our major conclusion is that, even using the integral formulation with full ion-Larmor-radius effects, the collisionless universal eigenmode is absolutely stable. In the course of our investigation, we have developed a general stability theory employing the S-matrix technique in the complex x plane, which may have wider applicabilities.

Our method for analysing the stability of drift-wave eigenmodes with arbitrary radial wavelengths is an extension of the S-matrix technique [6] for the differential formulation. Briefly stated, the method consists of introducing a real parameter λ which varies from 0 to 1 such that $\lambda = 1$ corresponds to the original integral equation and $\lambda = 0$ corresponds to the differential equation approximation which has been shown [1, 7] to allow only damped eigensolutions. We then formulate the problem as a scattering one and show that the scattering amplitude contains no poles on the real ω axis for all real λ between 0 and 1. Care must be taken to ensure that no additional unstable

* New address: Lawrence Livermore Laboratory, M-Division, L-439, P.O. Box 808, Livermore, CA 94550, USA.